In search of a broader microscopic underpinning of the potential energy surface in heavy deformed nuclei

IOP Conf. Series: Journal of Physics: Conf. Series **876** (2017) 012012 doi:10.1088/1742-6596/876/1/012012

In search of a broader microscopic underpinning of the potential energy surface in heavy deformed nuclei

P. O. Hess[1], M. Ermamatov[2]

[1]Instituto de Ciencias Nucleares, UNAM, Circuito Exterior, C.U., A.P. 70-543, 04510 México D.F., Mexico
[2]Instituto de Fisica, Universidade Federal Fluminense, 24210-340, Niteroi, Rio de Janeiro, Brazil
and
Theoretical Physics Department, National University of Uzbekistan, Tashkent, Uzbekistan

E-mail: [1]hess@nculeares.unam.mx ,[2]mirshod.ermamatov@if.uff.br

Abstract. Starting from the content of the shell model space and using a simple symplectic as a weight Hamiltonian, the relative positions of different symplectic irreducible representations are deduced. Applying a geometrical mapping leads to a microscopically derived *Potential-Energy-Surface*. After smoothing this surface and fitting a mass parameter to the first excited 6^+-state in the ground state band, the spectrum of a nucleus can be reproduced qualitatively. The method is also used to obtain a first estimation of the quadrupole Potential Energy Surface of any nucleus, allowing to obtain information about the structure of the nucleus in question. Of special interest is the prediction of the structure of nuclei away from the valley of stability and of super-heavy nuclei. The method will be illustrated at ^{184}W. One objective is to show that the *Pauli Exclusion Principle* is the main driving force for the structure of a nucleus, though some further microscopic input has to be used.

1. Introduction

The main objective is to show that by a minimal number of assumptions the *Potential Energy Surface* (PES) of quadrupole deformations of a nucleus can be guessed and that the resulting spectrum is near to the observed one. This enables us also to obtain a first hint to the collective quadrupole structure of super-heavy nuclei and of nuclei not measured yet.

The minimal assumptions are:

1) The use of the shell model space, sub-divided into irreducible representations (irreps) of the symplectic group [1]. The result is the consequence of the *Pauli Exclusion Principle* and up to here the procedure is fully microscopic.

2) The use of a simple test-Hamiltonian, which traces the relative distance in energy of the symplectic irreps. Here enters the importance of the quadrupole.quadrupole interaction, which drives the deformation. This test-Hamiltonian only serves to set the relative weight, position in energy, for each symplectic irrep. The test-Hamiltonian by no means is a microscopic Hamiltonian with all possible contributions needed for a full treatment. As we will see, some

important microscopic information will be hidden in two parameters, namely in the experimental deformation of the nucleus and in the mass parameter.

This alone will enable us to get a first guess on the PES. Further steps are:
3) Because we have not the possibility to diagonalize the Hamiltonian with an arbitrary potential, one has to obtain a PES within the *General Collective Model* (GCM) [2, 3], fitting it to the microscopically derived PES, which will introduce errors.
4) If a state within the ground state band is known, fitting the mass parameter B_2 [2] to this state, if possible with a large angular momentum. The parameter B_2 will adjust the moment of inertia. This parameter hides the contribution from, e.g., the nucleons in the intruder levels.

One main objective of this contribution is that the observation of the *Pauli Exclusion Principle* is the most important ingredient to obtain the information about the structure of a nucleus. Knowing the number of protons/neutrons in their valence shell determines which $SU(3)$ irreps are possible and, thus, the structure of the nucleus.

In this contribution we will illustrate the method at the example of ^{184}W and at ^{252}No.

The paper is organized as follows: In Section 2 we will present the sketch of the procedure, in section 3 it will be applied to ^{184}W and in Section 4 conclusions will be drawn.

2. The procedure

An important ingredient is the symplectic model of the nucleus [1] and its contracted version (see, for example [4]). More details can be retrieved in [5] on which also this contribution is based. In [6] the main steps on how to obtain the microscopically derived PES is explained for the first time and applied to ^{238}U.

The main points are that for heavy nuclei the symplectic irreps for the proton and neutron part are obtained separately. After that, it suffices to use a linear coupling of the proton and neutron irreps, because those are lower in energy as the non-linear coupled ones (which correspond to giant resonances). As a Hamiltonian, which provides a relative weight to each irrep, we use one from the contracted symplectic model [4]:

$$H = \hbar\omega\tilde{N} - \frac{1}{2}\chi\left[Q^c \cdot Q^c - (Q^c \cdot Q^c)_{shell}\right] \quad , \tag{1}$$

where $\tilde{N}$ is the phonon number operator of the protons plus the neutrons, $\hbar\omega$ is $45A^{1/3}$-$25A^{2/3}$ MeV for light and $41A^{1/3}$ MeV for heavy nuclei. The tilde refers to the use of the pseudo-$SU(3)$-model [7, 8], see also further below. The Q^c_m is the physical quadrupole operator and $(Q^c \cdot Q^c)_{shell}$ is the *trace equivalent part* of the quadrupole-quadrupole interaction, which guarantees that even for large deformation in average the shell structure is conserved [9]. The nucleons are filled into the Nilsson orbitals at a deformation given by [10] or by experiment, thus, microscopic information enters which is treated here as a black box. The χ-parameter is determined such that the lowest symplectic irrep has its minimum at the deformation value used as an input.

The symplectic Hamiltonian alone works well when the nucleus is well deformed, i.e., there is one dominant symplectic irrep to which one can restrict. However, for a general nucleus there are strong mixing of the symplectic irreps, which have to be taken into account, when a full microscopic treatment is applied. Here, we want to show by the results that the test-Hamiltonian is sufficient to get an estimate of the relative influence of the symplectic irreps. The mixing will be implicitly taken into account, as will be mentioned further below.

The mapping to a geometrical potential is performed defining first a vector coherent state [11] $\mid \Phi(\alpha_{2\mu})\rangle$, which is given by an operator being an exponential function in the symplectic operators which raise the number of phonons by two, applied to a lowest weight state of an $\widetilde{SU}(3)$ irrep within the valence shell. The $\alpha_{2\mu}$ defines the quadrupole variable. The geometrical

potential is the obtained through the expectation value of the Hamiltonian with respect to this vector coherent state. Note, that the shell model space is well defined and is subject to the *Pauli Exclusion Principle*. The content is only determined by the number of protons and neutrons, distributed along the shell model orbitals. The number of active nucleons for light nuclei is represented by all the nucleons, while for heavy nuclei the pseudo-$SU(3)$ is used [7, 8]. In the pseudo-$SU(3)$ shell model the orbitals are divided into *unique* and normal ones, where the *unique* orbitals are all those with the largest spin in each shell and the *normal* ones are all others. The angular momentum $l = j \pm \frac{1}{2}$, within the standard shell model, are redefined to $\tilde{l} = j \mp \frac{1}{2}$ and the content of a former shell with η oscillation quanta is mapped to a pseudo shell $\tilde{\eta} = \eta - 1$. In order to obtain the information of how many protons and neutrons are occupying the *normal orbitals* one needs the information on the deformation (which contains microscopic information) and fill in the nucleons at this deformation within the Nilsson diagrams from below. This division into two different kinds of orbitals is by no means sufficient. The intruder orbitals are important, for example, to get the moment of inertia right. However, this we treat as a parameter and the effects of the intruder orbitals are implicitly taken into account.

Restricting to *only one* symplectic irrep, in lowest order the potential is given by

$$\begin{aligned} V &\approx \frac{65}{16\pi}(\chi N_s^2)\tilde{\beta}_s^2 + \frac{5}{4\pi}N_s\left(\hbar\omega - \frac{7}{6}\chi N_s\right)(\tilde{\beta} - \tilde{\beta}_s)^2 \\ &- (\chi N_s^2)\frac{5}{\pi}\tilde{\beta}_s\tilde{\beta} + \frac{5}{2\pi}N_s\left(\hbar\omega + \frac{5}{6}\chi N_s\right)\tilde{\beta}_s\tilde{\beta}\,(1 - \cos(\gamma - \gamma_s)) \quad , \end{aligned} \tag{2}$$

where $\tilde{\beta}_s$ is related to a particular pseudo-$SU(3)$ irrep $(\widetilde{\lambda}, \widetilde{\mu})$ via

$$\tilde{\beta}_s = \left[\left(\frac{4\pi}{5N_s^2}\right)\left(\widetilde{\lambda}^2 + \widetilde{\lambda}\widetilde{\mu} + \widetilde{\mu}^2 + 3\widetilde{\lambda} + 3\widetilde{\mu}\right)\right]^{\frac{1}{2}} \quad . \tag{3}$$

The N_s is the total number of phonons in the lowest pseudo-$SU(3)$-state plus $3\frac{(\tilde{A}-1)}{2}$ and $\tilde{\beta} = \frac{\beta}{\kappa}$ ($\tilde{\beta}_s = \frac{\beta_s}{\kappa}$). (In [6] the factor $\frac{1}{\kappa}$ was omitted for β_s for heavy nuclei, which does not lead to significant deviations for prolate nuclei but being important for the case of oblate nuclei.) The value κ is approximately given by $\frac{1}{2}(\frac{\tilde{\eta}_p+1.5}{\tilde{\eta}_p+0.5} + \frac{\tilde{\eta}_n+1.5}{\tilde{\eta}_n+0.5})$ with $\tilde{\eta}_p$ and $\tilde{\eta}_n$ being the pseudo valence shell number for protons and neutrons respectively. $(\tilde{\beta}_s, \gamma_s)$ in (2) is related to the deformation of the symplectic band head in the $0\hbar\omega$ [4] (see also Eq. (3)). The total PES is then obtained by the envelope of all potentials related to the sum of all symplectic irreps. Note, that the determination of the microscopic potential has no free parameters. By taking the envelop, we implicitly assume that the system can change from one potential of the type (2) to another one, when the last becomes lower. In the symplectic model as such, there are no transitions between different potentials. This means that the procedure proposed implies a more general Hamiltonian.

For the GCM collective potential we use [2]

$$\begin{aligned} V &= \frac{C_2}{\sqrt{5}}\beta^2 - \sqrt{\frac{2}{35}}C_3\beta^3\cos(3\gamma) + \frac{C_4}{5}\beta^4 - \sqrt{\frac{2}{175}}C_5\beta^5\cos(3\gamma) \\ &+ \left(\frac{2}{35}\right)C_6\beta^6\cos^2(3\gamma) + \frac{D_6}{5\sqrt{5}}\beta^6 \quad . \end{aligned} \tag{4}$$

The potential parameters are approximately deduced by fitting (4) to (2).

β_0 [12]	κ	$\widetilde{N}_{\rm vp}$	$\widetilde{N}_{\rm vn}$	$\widetilde{\eta}_{\rm p}$	$\widetilde{\eta}_{\rm n}$	$\widetilde{A}_{\rm p}$	$\widetilde{A}_{\rm n}$	$\widetilde{A}$	$N_{\rm s}$
-0.2344(17)	1.25	14	20	3	4	34	60	94	381.5

Table 1. The values of quantities used in the calculation of microscopic PES ^{184}W. The κ is a scale factor appearing in the mapping of $SU(3)$ to pseudo-$SU(3)$. $\widetilde{N}_{\rm vp}$ are the number of valence protons in the pseudo-valence shell $\widetilde{\eta}_{\rm p}$ and similar for the neurons. $\widetilde{A}_{\rm p}$is the number of protons in the normal orbitals and $\widetilde{A}_{\rm n}$ the same for the neutrons. $\widetilde{A}$ is the total number of nucleons in normal orbitals. Finally, $N_{\rm s}$ is the number of quanta of the normal orbitals in the pseudo-$SU(3)$ plus $\frac{3}{2}(\widetilde{A}-1)$.

C_2	C_3	C_4	C_5	C_6	D_6	B_2
-521.77	-337.80	14306.01	-502.64	1902.26	-60439.94	112.697

Table 2. The values of the phenomenological potential parameters for ^{184}W, determined by fitting.

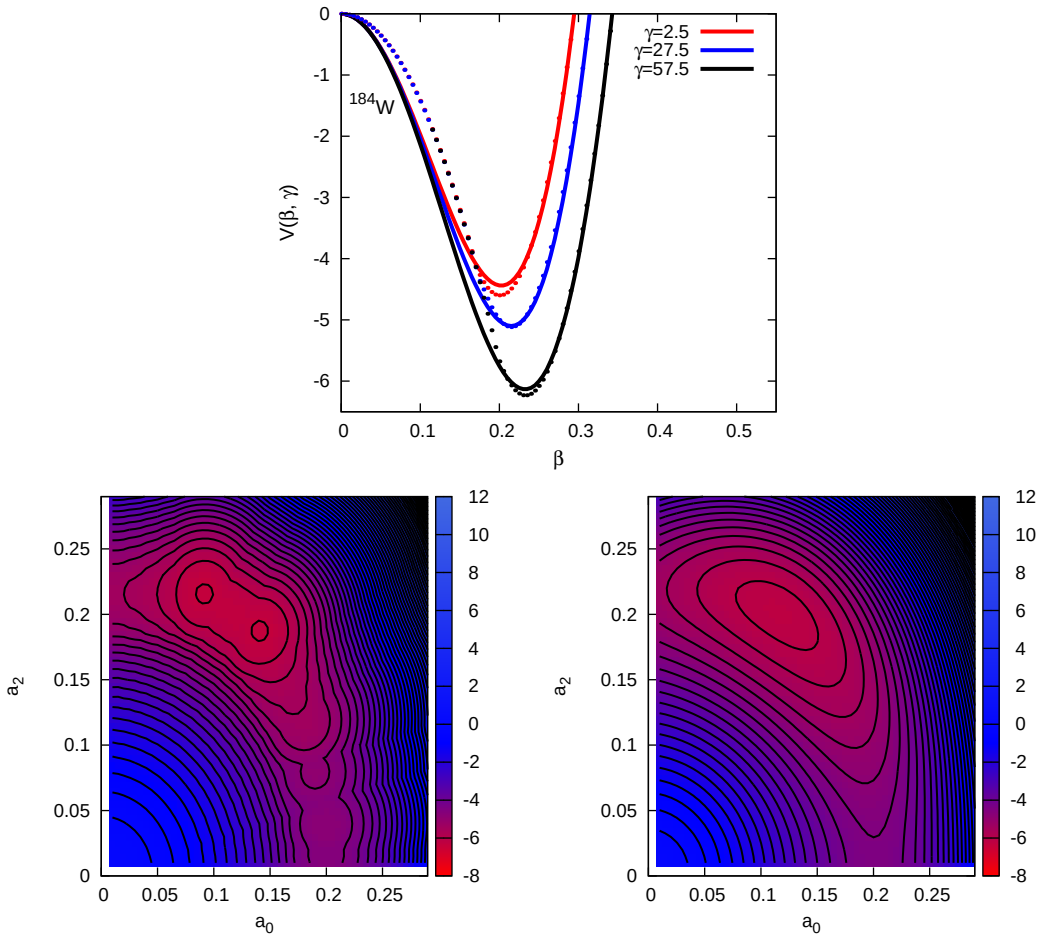

Figure 1. Comparison of microscopic and phenomenological potential energy surfaces of ^{184}W.

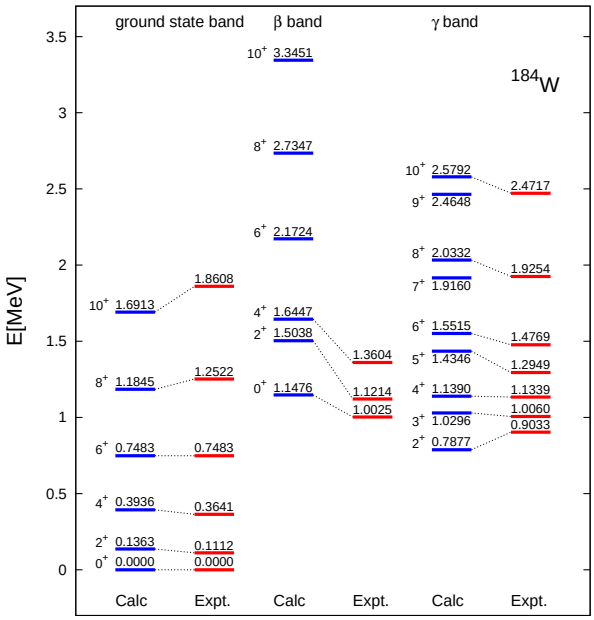

Figure 2. Comparison of the calculated energy levels ^{184}W with experimental data.

$L_{gs} \rightarrow L'_{gs}$	B(E2)		$L_{\beta} \rightarrow L'_{\beta}$	B(E2)		$L_{\gamma} \rightarrow L'_{\gamma}$	B(E2)	
	Calc	Exp		Calc	Exp		Calc	Exp
$0^+ \rightarrow 2^+$	1.95	3.78(6)	$0^+ \rightarrow 2^+$	1.68	-	$2^+ \rightarrow 3^+$	0.75	-
$2^+ \rightarrow 4^+$	1.06	1.86(5)	$2^+ \rightarrow 4^+$	0.07	-	$2^+ \rightarrow 4^+$	0.59	-
$4^+ \rightarrow 6^+$	1.01	1.63(5)	$4^+ \rightarrow 6^+$	0.55	-	$3^+ \rightarrow 4^+$	0.38	-
$6^+ \rightarrow 8^+$	1.03	1.5(3)	$6^+ \rightarrow 8^+$	0.78	-	$3^+ \rightarrow 5^+$	0.66	-
						$4^+ \rightarrow 5^+$	0.29	-
						$4^+ \rightarrow 6^+$	0.83	-
						$5^+ \rightarrow 6^+$	0.18	-
						$5^+ \rightarrow 7^+$	0.85	-
						$6^+ \rightarrow 7^+$	0.14	-
						$6^+ \rightarrow 8^+$	0.94	-
						$7^+ \rightarrow 8^+$	0.10	-

Table 3. Calculated intraband B(E2) values in e^2b^2 unit with experimental data for ^{184}W. Units are in e^2b^2.

$L_{\rm gs} \to L_\beta$	B(E2)		$L_{\rm gs} \to L_\gamma$	B(E2)		$L_\gamma \to L_\beta$	B(E2)	
	Calc	Exp		Calc	Exp		Calc	Exp
$0^+ \to 2^+$	29.4	-	$0^+ \to 2^+$	222.3	-	$2^+ \to 2^+$	0.9	-
$2^+ \to 2^+$	0.7	-	$2^+ \to 2^+$	175.0	-	$2^+ \to 4^+$	134.8	-
$2^+ \to 4^+$	1.6	-	$2^+ \to 3^+$	114.0	-	$4^+ \to 4^+$	245.7	-
$4^+ \to 4^+$	2.9	-	$2^+ \to 4^+$	17.0	-	$4^+ \to 6^+$	23.2	-
$4^+ \to 6^+$	1.1	-	$4^+ \to 4^+$	165.5	-	$6^+ \to 6^+$	262.4	-
$6^+ \to 6^+$	2.7	-	$4^+ \to 5^+$	60.0	-	$6^+ \to 8^+$	8.9	-
$6^+ \to 8^+$	0.8	-	$4^+ \to 6^+$	5.9	-	$8^+ \to 8^+$	256.3	-
$8^+ \to 8^+$	2.6	-	$6^+ \to 6^+$	154.5	-			-
			$6^+ \to 7^+$	40.2	-			-
			$6^+ \to 8^+$	3.1	-			-
			$8^+ \to 8^+$	145.5	-			-

Table 4. Calculated interband 10^3·B(E2) values in e^2b^2 units for ^{184}W. Units are in e^2b^2.

The procedure dos not provide us within information on ground state energies and related observables of the ground state of a nucleus. However, it can provide information on stability: A spherical PES hints to a particular stable configuration.

3. Applications

Due to lack of space, we simply resume the main results, as the energy spectrum, the structure of the PES and some transition values. The parameter values can be retrieved from the Tables 1 and 2 .

In the presentation of the conference the results for ^{182}W, ^{184}W and ^{186}W were presented. In this written version, only the ^{184}W-isotopes is considered. Experimental data were taken from [12]. This contribution serves to show the basic procedure. Applications to other known nuclei and super-heavy nuclei are published in [5]. The deduced microscopic potential has an immediate consequence on stability considerations of super-heavy nuclei: When the PES is spherical it clearly indicates stability. As can be seen from Figure 1, the GCM potential reproduces satisfactorily the microscopic derived one. In Figure 2 the spectrum is comparable to the experimental one, though the staggering within the sidebands is exaggerated. This was also observed in [5], where many different isotope chains were considered, including in the range of super-heavy nuclei. The agreement to the $B(E2)$ transitions within bands (see Table 2) are quite well predicted. A general feature is the exaggerated staggering within the vibrational bands.

Also a better agreement can be obtained using the deduced microscopic potential and not the approximation to the GCM-potential. However, in this case one needs a numerical routine [13], which is not available anymore.

An improvement in reducing the staggering within the vibrational bands can be achieved introducing a $1/\beta^2$ interaction as done in the Davidson potential [14], which implies however an additional parameter. Currently, we are including this interaction.

Finally, in Fig. 3 we present an example of a super-heavy nucleus. Only the PES is shown, while the spectrum can be retrieved in [5]. Many more have been considered in [5]. The particular example chosen is due to the knowledge of the states within the ground state band, which helps us to determine the mass parameter.

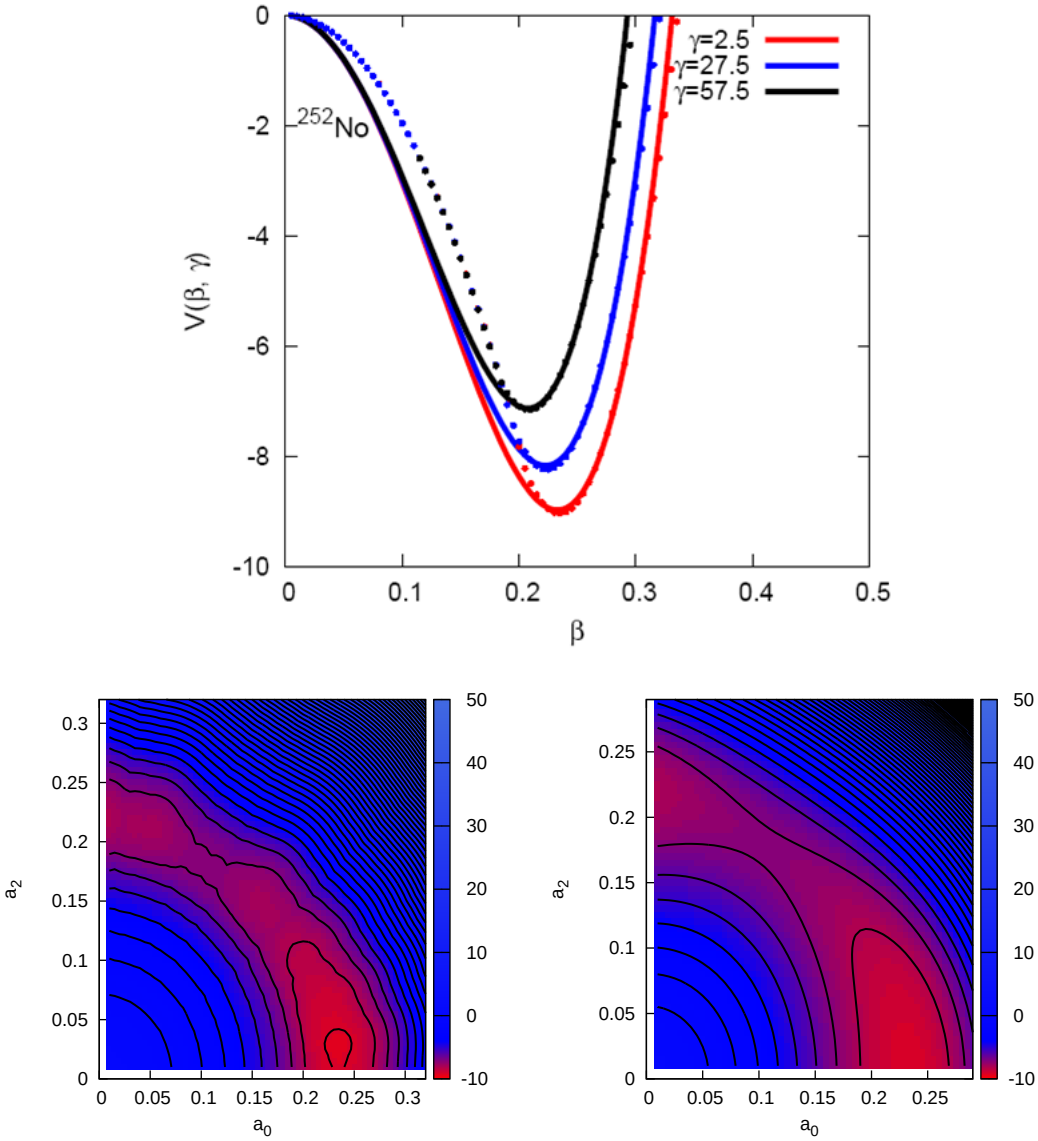

Figure 3. Comparison of microscopic and phenomenological potential energy surfaces of the super-heavy nucleus ^{252}No.

4. Conclusions

We estimated the structure microscopic PES with a minimum of physical assumptions and no free parameters, leading to the prediction of the collective quadrupole structure of nuclei in a wide range of heavy nuclei. The driving force for the structure is the *Pauli Exclusion Principle*, though further microscopic input are hidden in the information of the deformation (taken from experiment or the tables [10]) and the use of a weight Hamiltonian whose origin is the symplectic model. The symplectic model Hamiltonian is only used as a weight to obtain the order of the relative distance of the symplectic irreps, a difference due to the quadrupole-quadrupole interaction.

Finally, for the spectrum one fits the mass parameter to the energy of the first 6^+ state, or

one assumes a reasonable value. This also contains information on the microscopic structure, because it fits the moment of inertia.

As an illustrative examples we discussed the ^{184}W-isotope. The spectrum and $B(E2)$ transitions were calculated with a quite good agreement to experiment. A more complete presentation of the procedure was presented in the talk and especially can be found in [5].

Acknowledgment
The authors acknowledge financial help from DGAPA-PAPIIT (IN100315) and CONACyT (Project no. 251817). M.E. acknowledges financial support from the *Brazilian National Counsel of Technology and Scientific Development* (Project No. 165371/2015-3).

References

[1] D.J. Rowe, Rep. Prog. Phys. **48** (1985), 1419;
D.J. Rowe, Prog. Part. Nucl. Phys. **17** (1996), 265.
[2] P.O.Hess, M.Seiwert, J.A.Maruhn, W.Greiner, Zeitschr. f. Phys. **A296** (1980), 147.
[3] P.O.Hess, J.A.Maruhn, W.Greiner, Phys. **G7** (1981), 737.
[4] O. Castaños and J. P. Draayer, Nucl. Phys. A**491** (1989), 349
[5] M. Ermamatov and P. O. Hess, Ann. Phys. (N.Y.) **371** (2016), 125.
[6] O.Castaños, P.O.Hess, P.Rocheford, J.P.Draayer, Nucl. Phys. **A524** (1991),469.
[7] A. Arima, M. Harvey, and K. Shimizu, Phys. Lett. B **30**, (1969), 517.
[8] K. T. Hecht and A. Adler, Nucl. Phys. A **137** (1969), 129.
[9] G. Rosensteel and J. P. Draayer, Nucl. Phys. A**436** (1985), 445.
[10] P. Möller, J. R. Nix, W. D. Myers and W. J. Swiatetecki, Atom. Data and Nucl. Data Tab **59** (1995), 185.
[11] K. T. Hecht, *The vector Coherent Sate Method and its Application to Problems of Higher Symmetries*, Lecture Notes in Physics 290, (Springer, Heidelberg, 1997).
[12] www.nndc.bnl.gov/ensdf.
[13] D.Troltenier, J.A.Maruhn, W.Greiner, P.O.Hess, Zeit. f. Phys. A**343** (1992), 25.
[14] D. Bonatsos, E. A. McCutchan, N. Minkov, R. F. Casten, P. Yotov, D. Lenis, D. Petrellis, and I. Yigitoglu, Phys. Rev. C **76** (2007), 064312.